EAC 2015
2nd European Advanced Accelerator Concepts Workshop
13-19 September 2015 *La Biodola, Isola d'Elba*
Europe/Rome timezone

Mono-Energetic Ions emission by nanosecond laser solid target irradiation.

INFN Istituto Nazionale di Fisica Nucleare

Annamaria Muoio
LNS-INFN & Univ. degli Studi di Messina (Italy)

STVDIORVM VNIVERSITAS MESSANAE

Motivations

Investigate the acceleration mechanisms through Laser-matter interaction in ns domine

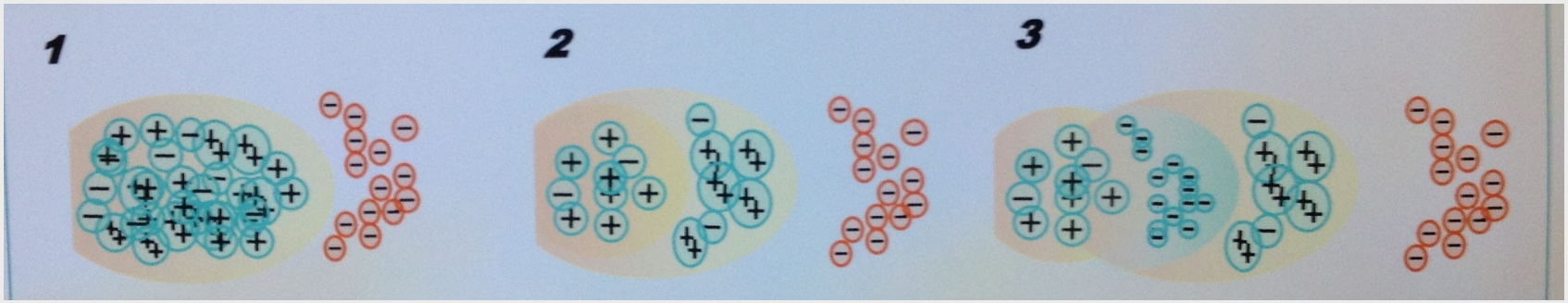

the plasma evolution can be depicted in the following way:

- prompt electrons escape rapidly, but not before they have repelled part of the electrons in the plasma bulk[1];

.

[1)] **Prompt electrons driving ion acceleration and formation of a two temperatures plasma in nanosecond laser-ablation domain**
D. MASCALI, et al. EPL

Increase inner plasma thermal energy….

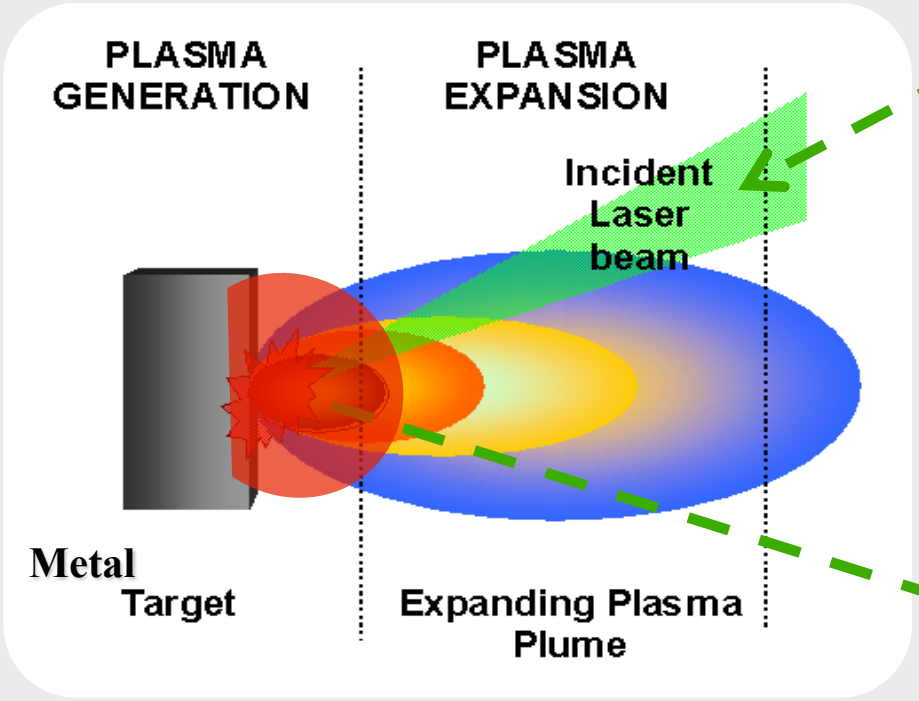

Normal Metal Target

- $I_{Reflected} > 90\%$!

New Target ?

It is almost a "total absorber" in the UV-VIS range.

Absorbance at λ=1064 nm MUST BE largest possible.

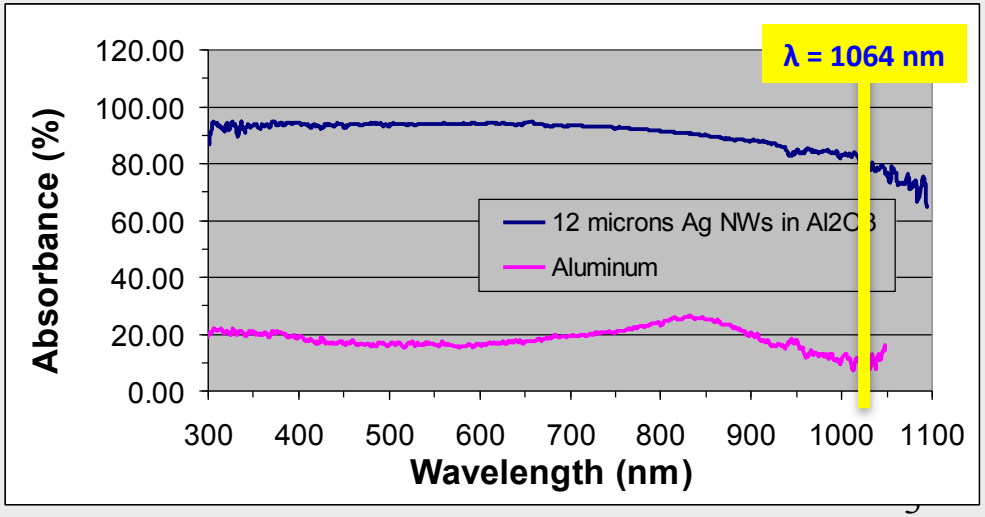

How we can Investigate ?

- Targets
- Experimental set-up
- and … DATA !

TARGETS

- Al (Pure Aluminum)
- Nano Targets (Al_2O_3 + Ag NWs)

Regular Nanostructur (Nano Wires)

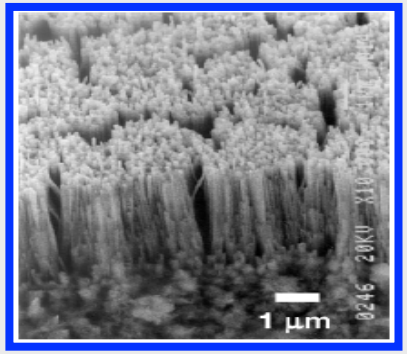

Example target
(after many laser-shots)

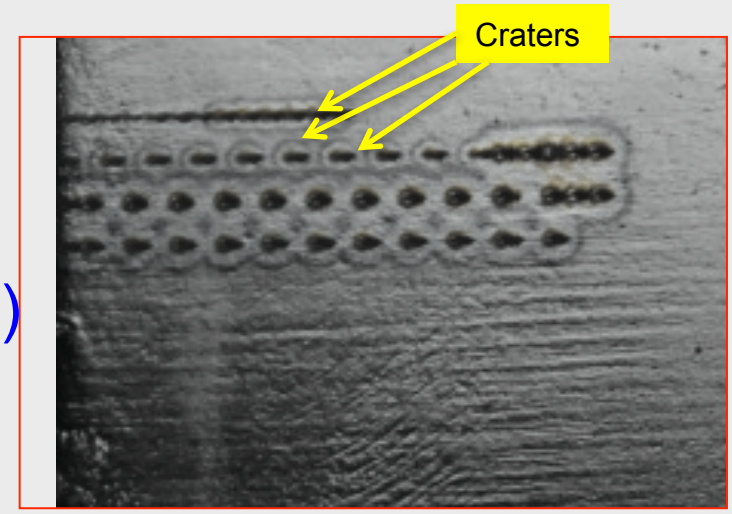

Experimental Set-Up (Lab LENS)

LASER:

Nd:YAG laser of Energy	**E_{max}=2,2 Joule**
Laser work modality	**0.8 - 1.2 - 2.0 J**
fundamental wavelength	**λ=1064 nm**
pulse-duration	**Δt=6 ns**
rep. Rate	**f=10 Hz**

Ions Collectors-ToF (IC)
placed at different angles to reconstruct the ions or electrons energies distribution.

ICCD (Intensified CCD) device acquire images in a small time widows (at list about 2 ns). Useful to study the time evolution of laser generated plasmas.

CCD for X-ray detection, for X-ray imaging (pinhole technique) and space-resolved X-ray spectroscopy

TPS, Thomson Parabola Spectrometer

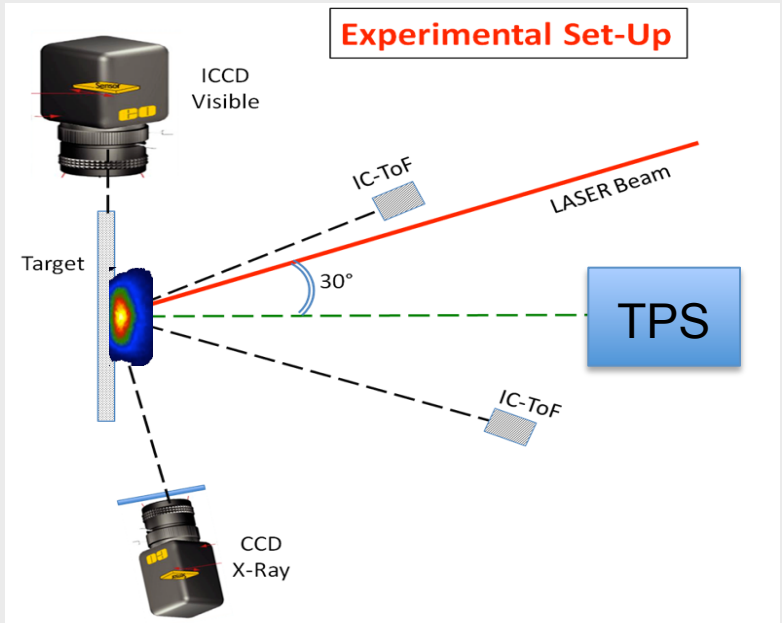

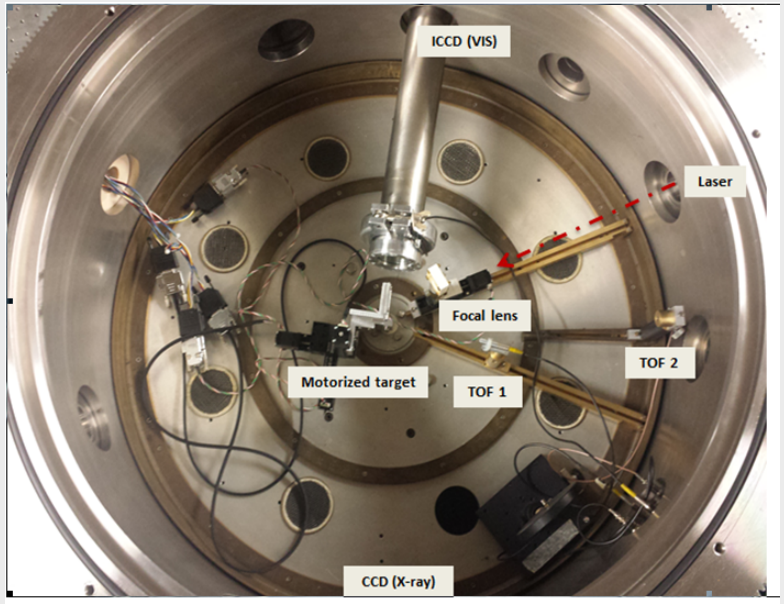

CCD for X-ray detection

The X-ray imaging of the plasma was obtained by using a X-ray sensitive camera coupled to a pinhole . The pinhole-camera (PHC) was fitted with a four-pinhole array (1 mm diameter) to allow a simultaneous 4-channel imaging, each channel was filtered to be sensitive to a different spectral region with Al thicknesses (2 μm, 7 μm, 10 μm, 20 μm).

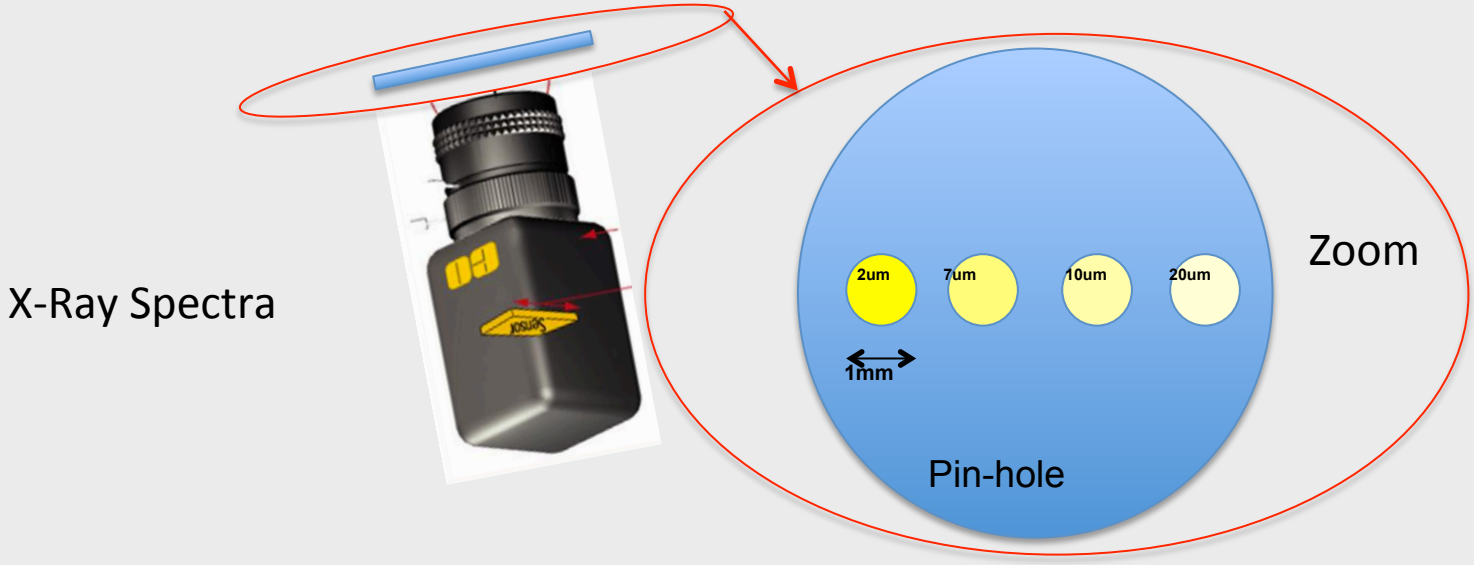

ICCD

Imaging VIS and flux measurement

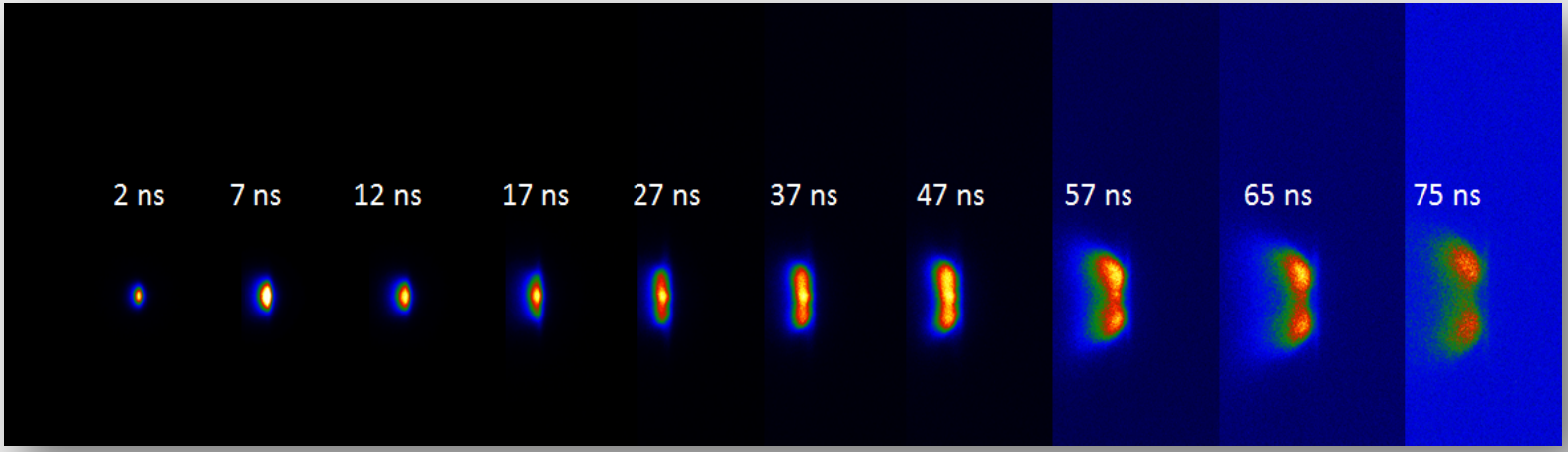

Time sequence of fast photography images showing the spatio-temporal evolution of the plasma plume recorded. The palette of the pictures is representative of the light intensity measured by the camera.

Fast photography using an ICCD provides two-dimensional snapshots of the three-dimensional plume propagation. This technique provides details of the expansion dynamics of the plasma. Higher counts observed in the images may correspond to areas of high temperature and particle density in the plasma plume. A minimum gate width of 2 ns was used at the earliest time of plasma evolution and the gate width value was gradually incremented to higher values to compensate reduced emission at later stages of the plume life. The plume is found to expand freely in vacuum and nearly spherical in nature.

THE THOMSON PARABOLA SPECTROMETER

In a TPS, ions with different charge-to-mass ratios are separated into distinct parabolas by means of parallel electric and magnetic fields.

TPS

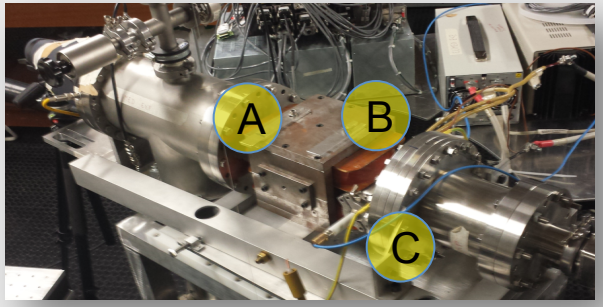

MCP

Detector
(Microchannel plate coupled to a phosphor screen and a camera)

CAMERA

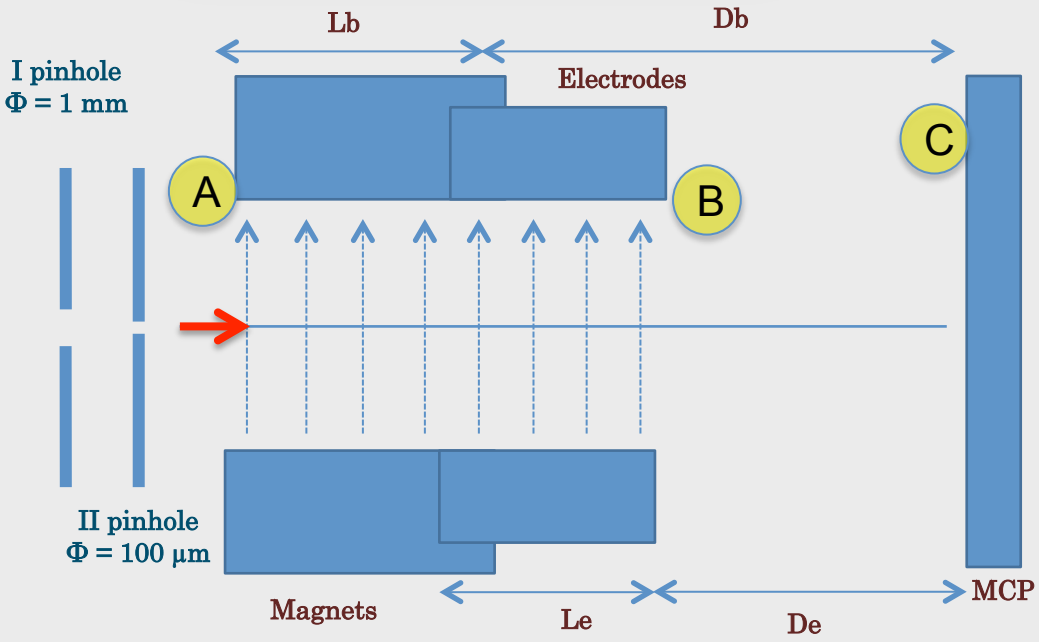

Parabolic traces on the detector screen

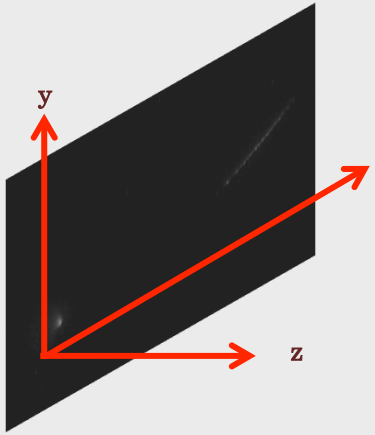

Experimental Data

From the diagnostics we have the following information:

a) **X-Ray Flux from CCD;**

b) **Optical (200-900nm) Flux from ICCD;**

c) **Ion velocities from IC-TOF.**

d) **Spectra from TPS**

We combine these experimental data to obtain Physical Information on Plasma.

From CCD

The X-Ray Flux as a function of four different Al attenuators thickness placed in front of the CCD sensor.

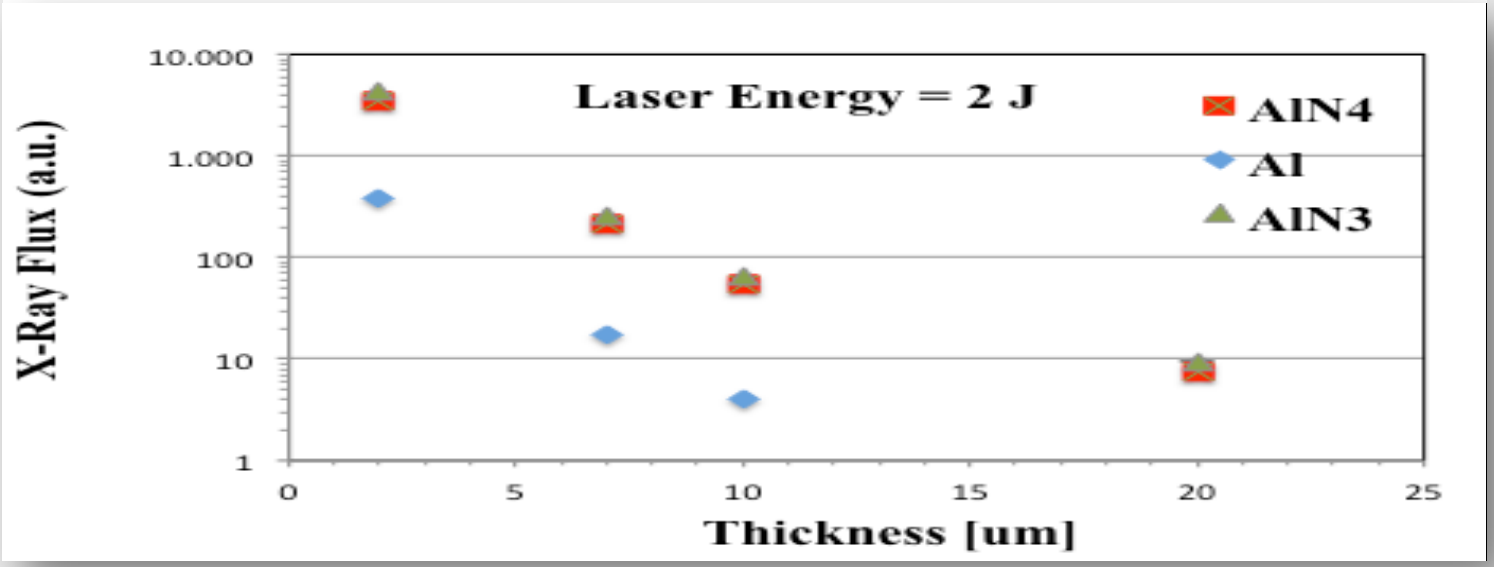

It can be noticed that for each thickness the flux impinging on the CCD is more than one order of magnitude larger when using Ag-NWs rather than pure Al targets.

This is a clear indication about the plasma energy content (i.e. the product between the density and the temperature) : it was much higher in the case of Ag-NWs targets

Relevant Results :

CLEAR EVIDENCE OF PLASMA STAGNATION DUE NWs TARGETS.

An evaluation of the temperature was carried out for Al and Ag-NWs Target: T_{Al}=0.15keV and T_{NWs}=0.6keV. → factor 4 of enanchement ! The density increases of a factor 2 approximately.

From ICCD

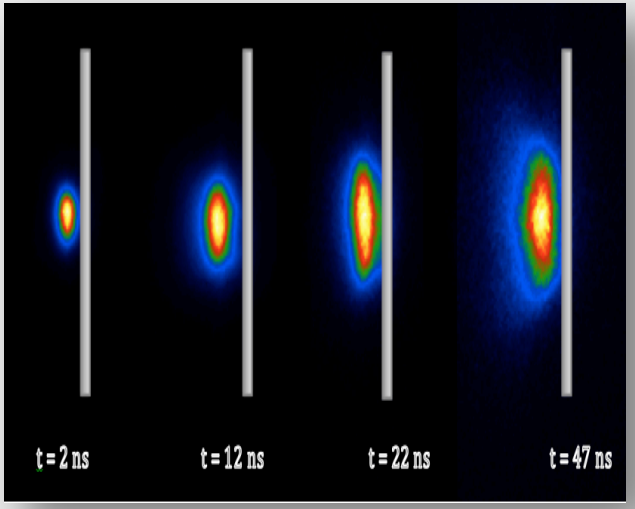

ICCD images of spatial distributions of the expanding plasma after 2ns, 12ns, 22ns and 47ns, displayed as a "false colour" image

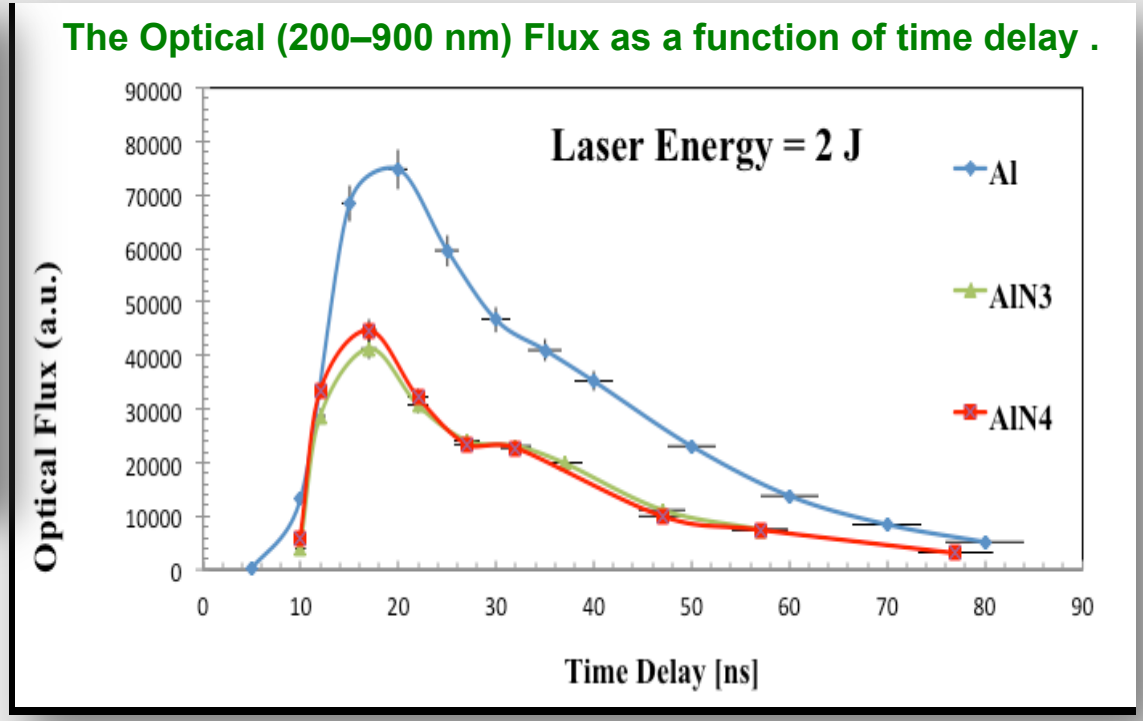

The Optical Flux coming out from the pure Al plasma **is three times larger** than Ag-NWs.

This result is an **additional confirmation** that the spectral energy of the plasma was upshifted towards larger and larger energies, and specifically towards EUV and X-ray domains.

From IC-TOF

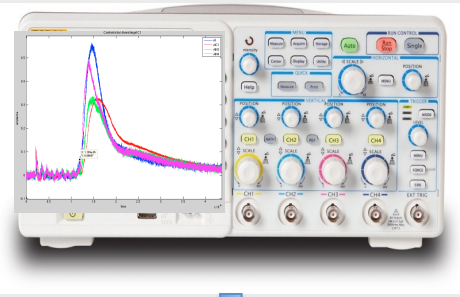

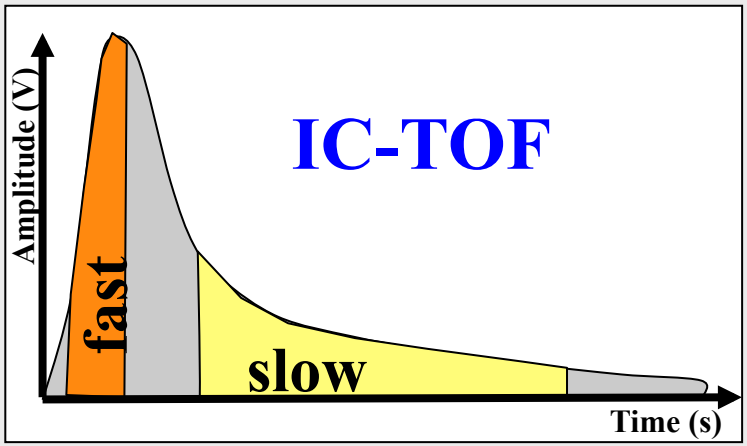

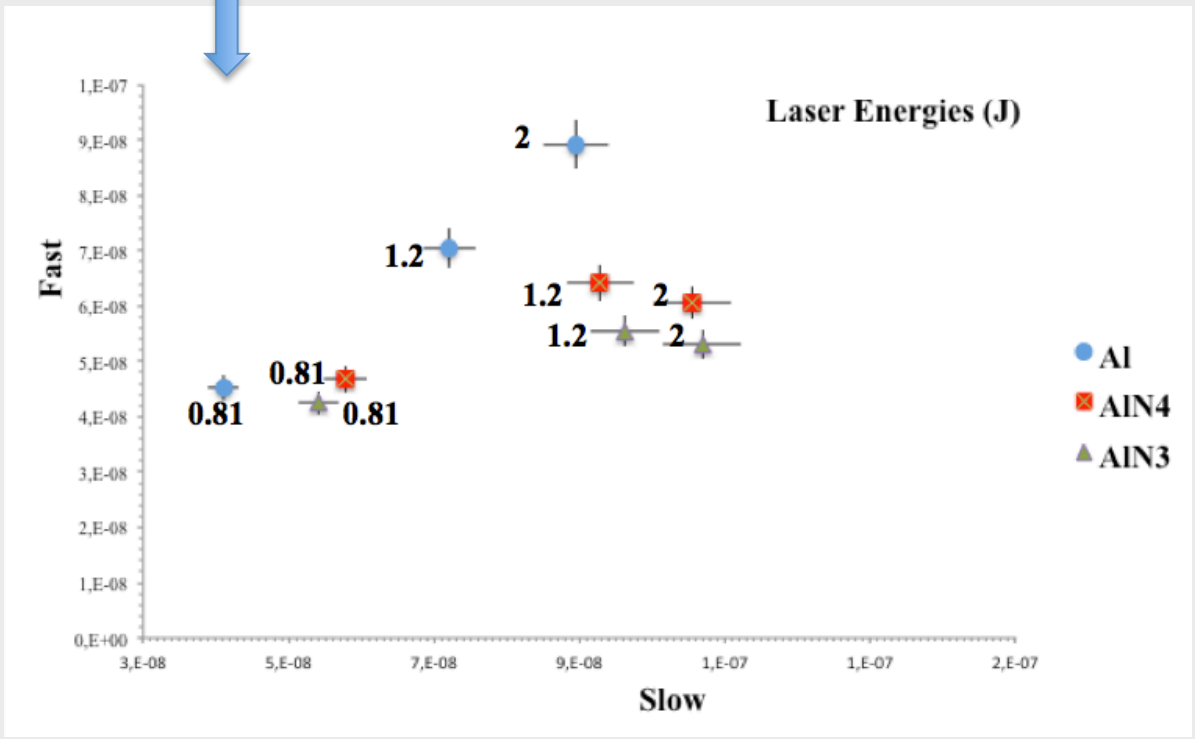

Temporal evolution at the different laser energies of both the fast-slow components is illustrated.

Increasing the laser energy We observe:

- Almost proportional enanchement for the Al-target ,
- saturate trend for the Ag-NWs targets.

relevant result
This is an additional confirmation

Related to the presence of **plasma stagnation** in the case of Ag-NWs targets.

(That means : laser energy is turned into thermal content of the plasma thus reducing the expansion velocity of the fast-plasma-component)

From TPS

Pure Al

Spectrograms from a 2 mm thick Al target at LENS laboratory.

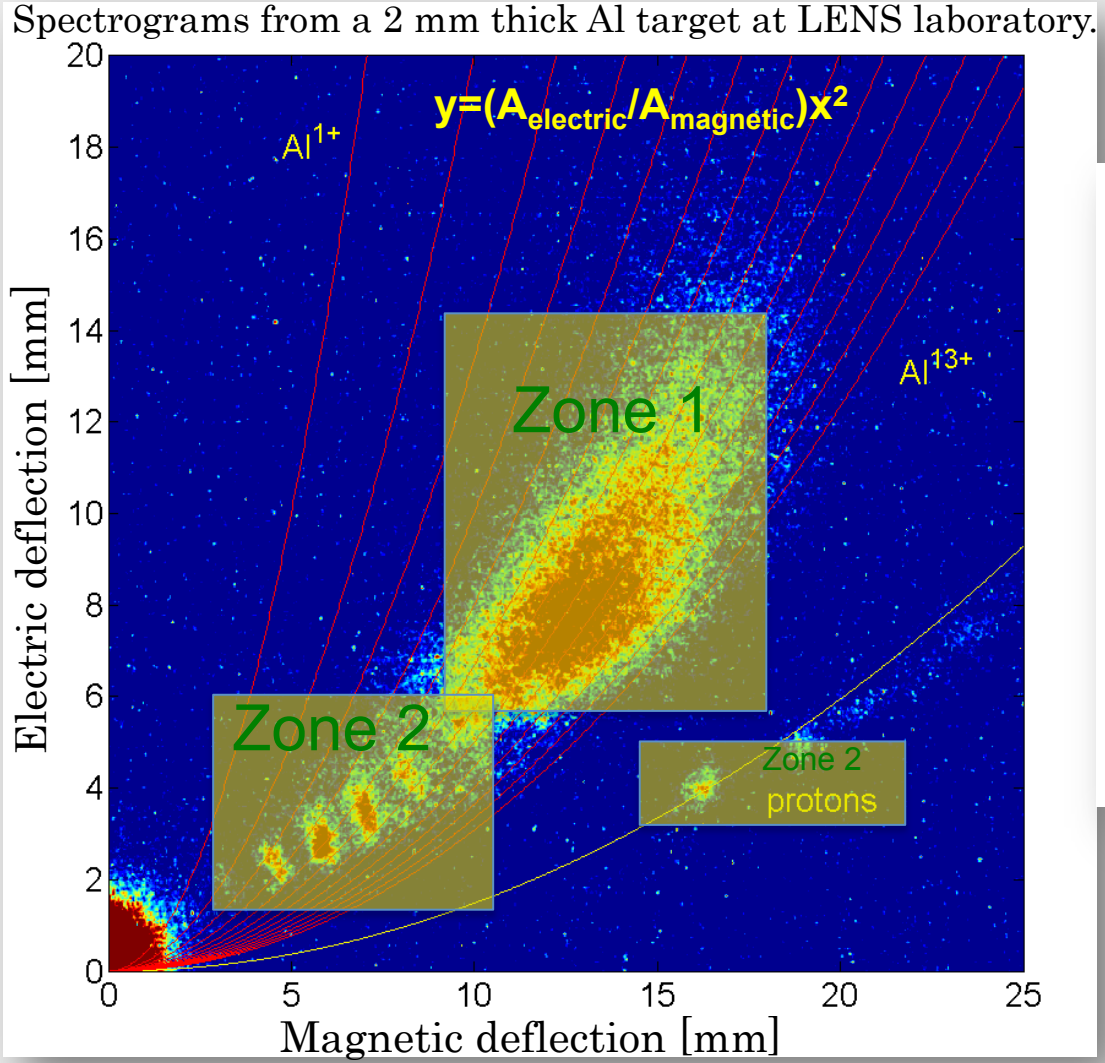

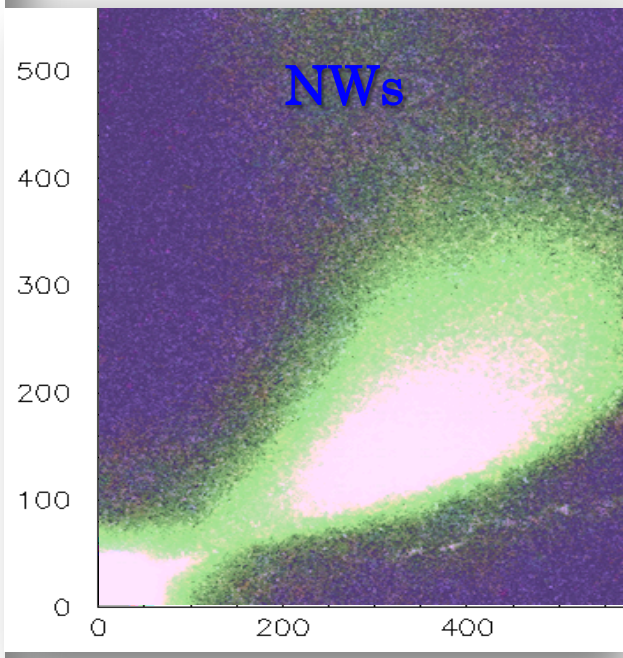

$K_E=A_{electric}/y$

$K_B=A_{magnetic}/x^2$

How we can study these zones ?

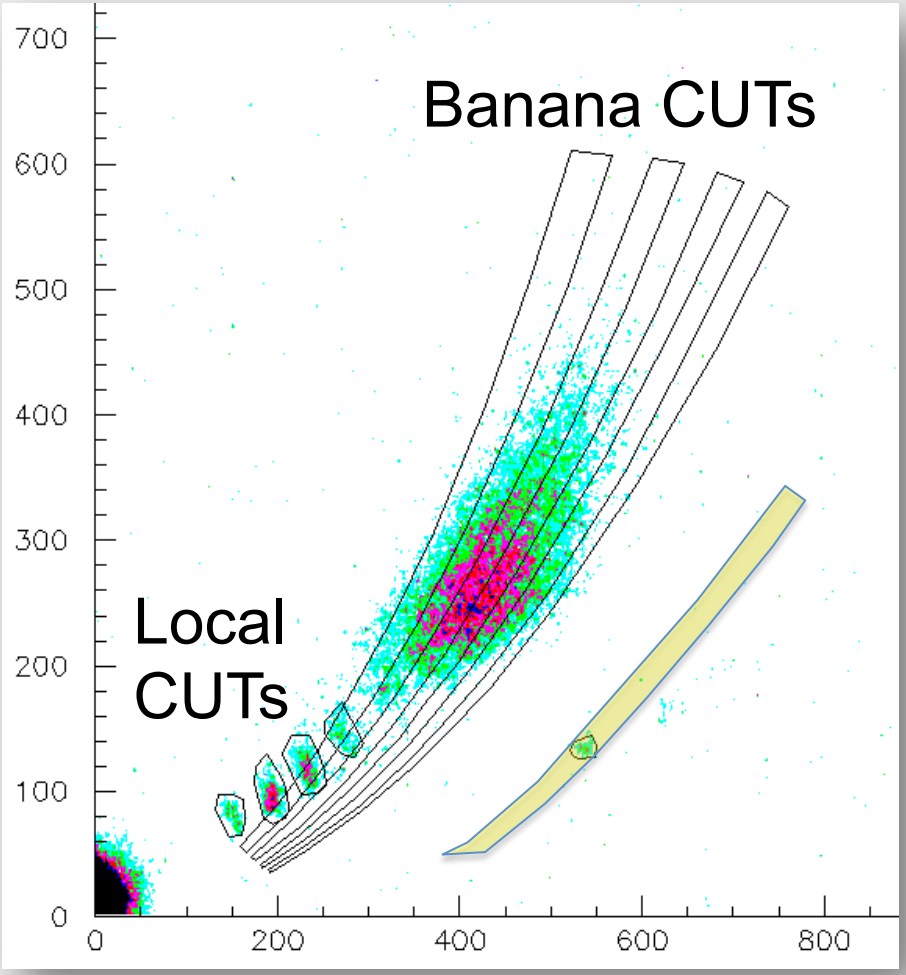

Spectra of different ion species and different charge states are constructed cutting out the parabolas as shown in figure.

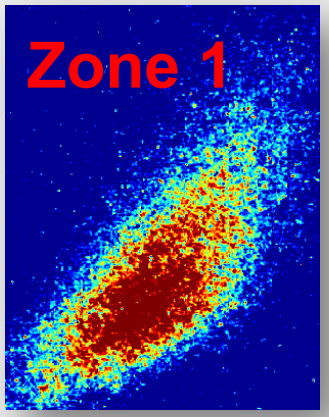

By fitting the spectra (log y & linear x) of the different ion species with a given charge state, one can calculate the **ionic temperature** from the linear fit parameter (slope of the curve).

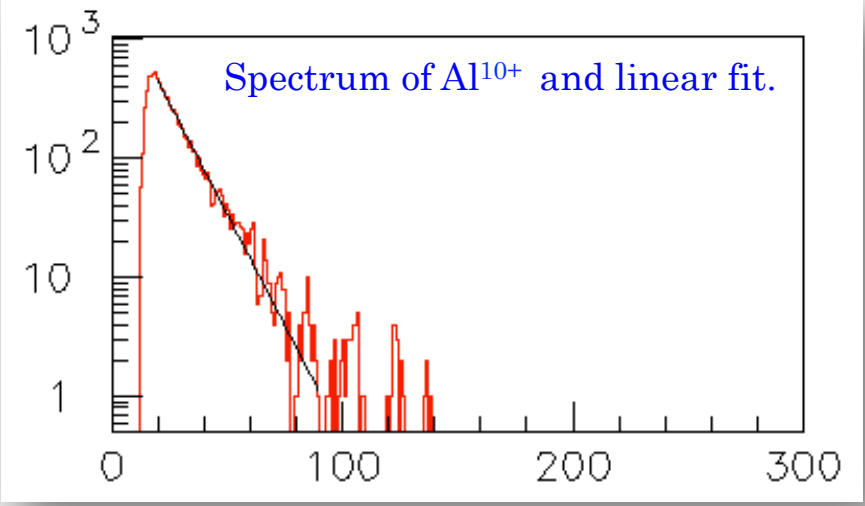

Ions	Temperature (keV)
Al^{9+}	11.9 ± 0.3
Al^{10+}	12.0 ± 0.4
Al^{11+}	11.7 ± 0.3
Al^{12+}	11.7 ± 0.3
Al^{13+}	13.8 ± 0.3

Temperature for different Al charge states.

Spectrum of monoenergetic Al charge states and protons.

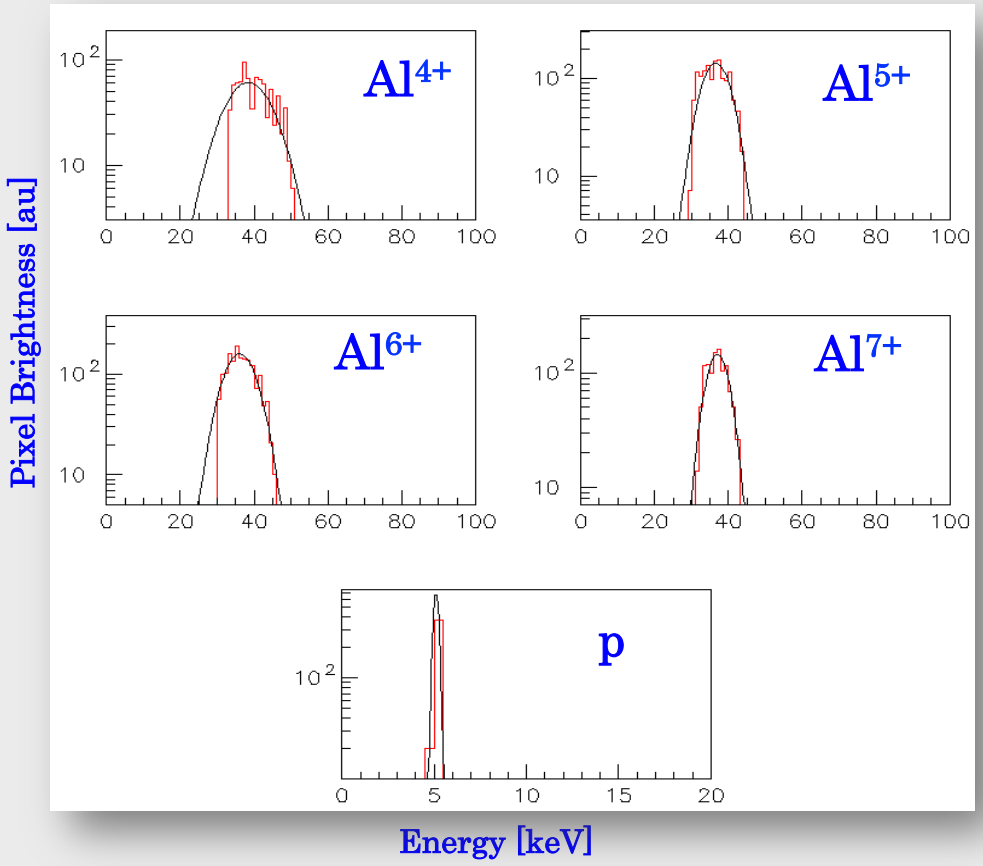

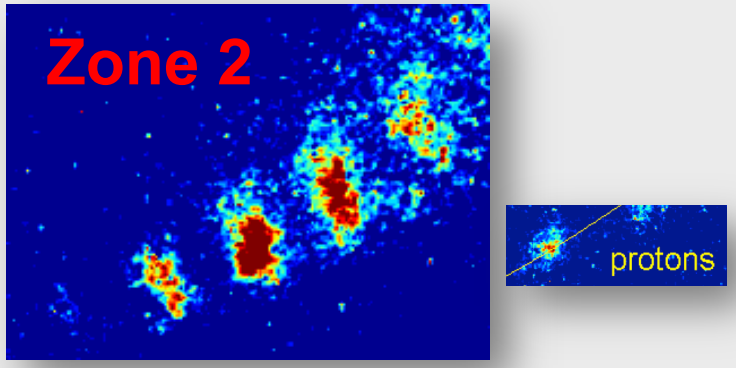

Energy of **protons** and **Al** charge states.

Ions	Energy (keV)
Al^{4+}	34.5 ± 6.2
Al^{5+}	35.6 ± 3.6
Al^{6+}	36.1 ± 4.2
Al^{7+}	37.0 ± 2.9
p	5.1 ± 0.1

It is possible to fit with **Gaussian function** the **mono-energetic** protons and different Al charge states. The maximum of spectra represents the value of the ions energy.

Conclusions

-At the reached values of fluence even when using ns lasers quasi mono-energetic protons and Aluminium ion beams can be generated. (The presented results are no singular occurrences, but represent a very stable and reproducible phenomenon.)

-The experiment demonstrates nanostructured targets have the effect **to increase the plasma energy content**, as observed by X-rays and optical diagnostic.

Such results are in agreement with the increment of absorption coefficients due to the specific structure of the target.

-**Signs of plasma stagnation**, of great interest for carrying out inner-plasma studies, have been found from the TOF data and surface analysis

… work in progress !!!


Thanks
Altana C. ,Lanzalone G., Mascali D.Tudisco,
Anzalone A., Caliri C., Cirrone GAP, Schillaci F.,
Odorici F. , Malferrari L.